Proceedings of the 10th International Chemical and
Biological Engineering Conference - CHEMPOR 2008
Braga, Portugal, September 4-6, 2008
E.C. Ferreira and M. Mota (Eds.)

Simulation of membrane separations using a modified Maxwell-Stefan model

Paulo Brito[1,2*], Licínio M. Gando-Ferreira[2], António Portugal[2]
[1] Chemical and Biological Technology Department, School of Technology and Management, Bragança Polytechnic Institute, Campus de Santa Apolónia, 5301–857 Bragança, Portugal
[2] CIEPQPF, Department of Chemical Engineering, University of Coimbra, Pólo II, 3030–790 Coimbra, Portugal

Keywords: Modeling, Ultra-filtration, Transport phenomena, Apparent rejection, Adaptive methods
Topic: Advancing the chemical and biological engineering fundamentals – Membranes and membrane science

Abstract

A modified Maxwell-Stefan model, which considers both the concentration polarization and the transport through the membrane, is tested for the simulation of Dextran-98000 aqueous solutions filtration.

The model is able to successfully simulate experimental data in the high rejection/low flux region, but does replicate the observed rejection drop/pressure build-up which occurs for increased fluxes, which may be due to limitations of the model itself.

1 Introduction

The modeling of mass transfer phenomena in solute separations through inert membranes is essential for the efficient design and optimization of these operations, namely ultra-filtration processes, widely applied in an important range of industries, that include food and biotechnological industrial processes. In this work, a model is applied to simulate the ultra-filtration of aqueous solutions, based on a particular aproach to the Maxwell-Stefan general equations (Kerkhof, 1996). The ultra-filtration process simulation provides an analysis of the solute rejection phenomenon, which, in general, depends on the solution components properties (namely, their molecular sizes), the membrane characteristics and the process operational conditions. Therefore, through the intramolecular transport modelation, we can quantify the influence of each former conditions in the refered rejection phenomenon. This strategy provided promising results in the simulation of PEG-3400 aqueous solutions ultra-filtration (Brito et al., 2004, Ferreira et al., 2003). Now, the purpose is to test the ultra-filtration simulation performance for more massive solutes, specifically dextran-98000.

2 Model

The model considers both the concentration polarization and the transport through the membrane and incorporates a binary friction model based on the Maxwell-Stefan-Lightfoot equation (Kerkhof, 1996). Hence, for the polarization layer, we have:

$$\frac{\partial c}{\partial t} = -\frac{\partial N}{\partial z} \tag{1}$$

with the flux, *N*, defined as,

* Corresponding author. Tel + 351-273-303110. E-mail:paulo@ipb.pt

$$N = -(D + D_t)\frac{\partial c}{\partial z} + u_v c \tag{2}$$

where, $D = D_{12}\Gamma_c$, being D, the Fickian diffusion coefficient; D_t, the turbulent diffusivity; D_{12}, the Maxwell-Stefan diffusion coefficient; and Γ_c, the thermodynamic factor. The turbulent diffusivity is defined assuming an unitary turbulent Schmidt number ($\mathrm{Sc_t} = \nu_t / D_t$), and taking account the turbulent cinematic viscosity computed by the Vieth correlation (Brito et al., 2004):

$$\frac{\nu_t}{\nu} = \left(\frac{2}{9}\pi\sqrt{3}\right)^3 \left(\frac{f}{2}\right)^{3/2} \left(y^+\right)^3 \tag{3}$$

with the normalized distance from the membrane wall, y^+, calculated by,

$$y^+ = \frac{y\langle u_t \rangle \sqrt{f/2}}{\nu} \tag{4}$$

being f, the Fanning friction factor, defined by the Blasius equation, $f = (0.3164/4)\mathrm{Re}^{-0.25}$, and u_t, the circulating fluid velocity.

For the membrane, on the other hand, the molar concentration temporal gradient is given by:

$$\varepsilon \frac{\partial c'}{\partial t} = -\frac{1}{\tau}\frac{\partial N_m}{\partial z} \tag{3}$$

in which, τ is the tortuosity factor, and ε is the porosity. The intramembrane flux, N_m, is calculated by:

$$N_m = -\frac{\Gamma_c}{G}\frac{\partial c'}{\partial z} + u_v \frac{F}{G} c' \tag{4}$$

where, F and G are the convective and friction factors respectively, defined as in Kerkhof (1996) for a monosolute system, with the solute and the solvent represented by subscripts 1 and 2, respectively:

$$F = \left(\frac{1}{D_{12}} + \frac{c_t{}^2 \overline{V}_1 \overline{V}_2}{B_o}\kappa_2\right)\frac{\tau}{\varepsilon} \tag{5}$$

$$G = \left(\frac{1}{D_{12}} + \frac{c_t}{B_o}\left(\phi_2 \kappa_1 \overline{V}_1 + \phi_1 \kappa_2 \overline{V}_2\right)\right)\frac{\tau}{\varepsilon} \tag{6}$$

where, c_t is the total molar concentration, $B_o = r_p^2/4$, is the permeability parameter, r_p, the porous radius, and $\overline{V}_i$, ϕ_i and κ_i are the molar volume, the volume fraction and the viscosity fractional coefficient of component i, respectively. The thermodynamic factor Γ_c is given by (Kerkhof, 1996):

$$\Gamma_c = 1 + c\frac{\partial \ln \gamma}{\partial c} - \frac{c}{c_t}\left(1 - \overline{V}_1 / \overline{V}_t\right)$$

However, ideality is assumed.

The model is completed by the definition of: boundary conditions, fixed bulk concentration at the polarization layer extreme, and equilibrium and flux equalization conditions at the membrane/polarization and membrane/permeate interfaces;

$$z = -\delta \quad \Rightarrow \quad c = c_b$$
$$z = 0 \quad \Rightarrow \quad c' = K_{eq} c \; ; N = N_m \tag{7}$$
$$z = L_m \quad \Rightarrow \quad c' = K_{eq} c_p \; ; N = u_v c_p$$

and initial conditions, zero concentration profile start-up,

$$t = 0 \quad \Rightarrow \quad c = c_b \quad (z = -\delta) \quad \wedge \quad c = c' = 0 \quad (z > -\delta) \tag{8}$$

The problem is discretized in the spatial direction and solved in the temporal dimension until a steady-state profile is reached, which implies a constant profile for the flux over all the spatial domain. Therefore, a simulated stationary permeate concentration, c_p, becames available, that can be used to calculate the apparent solute rejection, R_{app}:

$$R_{app} = 1 - {c_p}/{c_b} \tag{9}$$

The fluxes profiles allow the computation of the pressure drop due to the flow and the simulated total pressure drop,

$$\Delta P_{flow} = \frac{\tau}{\varepsilon} \frac{RT}{B_o} \int_0^{L_m} c_t \sum_{i=1}^{2} \kappa_i N_i \overline{V}_i dz \tag{10}$$

$$\Delta P_{total} = \Delta P_{flow} + \sigma \, \Delta\Pi \tag{11}$$

where $\Delta\Pi$ is the osmotic pressure drop through the membrane and σ, the osmotic reflection coefficient. The membrane resistence may be computed relating the flow pressure drop and the flux using pure water filtration experiments.

$$R_m = \frac{\Delta P_{flow}}{\eta_w u_v} \tag{12}$$

On the other hand,

$$R_m = \frac{L_m}{B_o} \frac{\tau}{\varepsilon} = \frac{8 L_m}{r_p^{\,2}} \frac{\tau}{\varepsilon} \tag{13}$$

which allows the estimation of relations between the structural properties of the membrane, namely of τ/ε, a critical model parameter.

For the particular monosolute system under study (dextran-1 and water-2), the following relations are used in the computation of the specified properties (Blox, 2003):

$$D = 5.96 \times 10^{-11} + 2.12 \times 10^{-11} \tanh(0.0284\rho - 1.491) \tag{14}$$

$$\Pi = 37.0\rho + 0.752\rho^2 + 76.4 \times 10^{-4} \rho^3 \tag{15}$$

and

$$\kappa_1 = \kappa_2 \left(1 + \frac{\eta_{sp}}{\phi_1} \right) \tag{16}$$

$$\kappa_2 = {\eta_w}/{c_t RT} \tag{17}$$

with,

$$\eta_{sp} = a\rho \exp(b\rho) \tag{18}$$

where, ρ represents the solution mass concentration.

3 Numerical Solution

The numerical solution of a normalized version of the partial differential-algebraic equation system, defined over a space-time coordinate system of variables, is accomplished with an adaptive resolution algorithm, based on the Adaptive Method of Lines, and presented by Brito and Portugal (1998). This method is used to solve simultaneously the two modules of the model (polarization layer and membrane) over a one-dimensional discretized space direction, in the time direction until a steady state solute concentration profile is reached. The spatial derivatives are approximated by central finite differences and the time integration is accomplished with DASSL numerical integrator. The normalized concentrations (y and y') are defined in relation to the bulk concentration, c_b, and the spatial coordinate ($-\delta \leq z \leq L_m$) is normalized to the total spatial domain extent:

$$z^* = \frac{z + \delta}{L_m + \delta} \tag{19}$$

being δ, the polarization layer size and L_m, the membrane thickness. The operational conditions, the solution components and membrane properties, and the simulation parameters used in the obtainance of all results presented in the next section, are resumed in Table 1.

Table 1. Operational conditions, properties, and simulation parameters.

Properties	Operational conditions and parameters
$\overline{V_1} = 45.6$ m^3/kmol	$\rho_b = 10$ kg/m^3
$\overline{V_2} = 0.018$ m^3/kmol	$u_t = 0.76$ m/s; 1.57 m/s
$L_m = 5\times10^{-7}$ m	$T = 298$ K
$r_p = 4.5\times10^{-9}$ m	$\delta = 86\times10^{-6}$ m
$\varepsilon = 0.5$	

4 Results

A typical run provides evolutionary profiles like the ones presented in Figures 1 and 2, for normalized concentration (y and y') and space (z^*) variables. The formation of significant solute accumulation at the membrane/polarization interface (in the presented case, the solute concentration is roughly four times higher than bulk concentration - c_b) is verified, together with diminished permeate concentrations, leading to high levels of apparent rejection of solute.

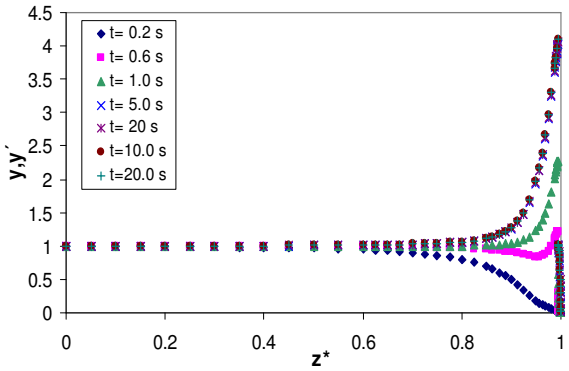

Figure 1. Normalized concentration profiles (polarization and membrane): u_t= 1.57 m/s, u_v= 1.0×10^{-5} m/s and K_{eq}= 0.25.

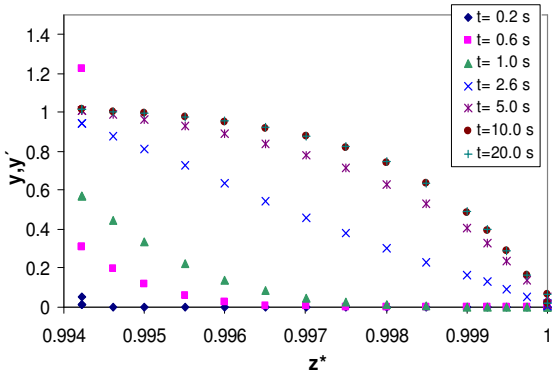

Figure 2. Normalized concentration profiles (membrane): u_t= 1.57 m/s, u_v= 1.0×10^{-5} m/s and K_{eq}= 0.25.

The large levels of rejection are maintained over a reasonable range of flux values (vd. Figure 3). It is verified that fixing K_{eq} at 0.25 allows a good agreement between experimental and simulated results in the practically constant rejection area. However, a sudden important decrease in rejection beyond a flux threshold is observed, which the model seems unable to

replicate, in spite of a slight decreasing tendency that does not fit at all to the experimental data.

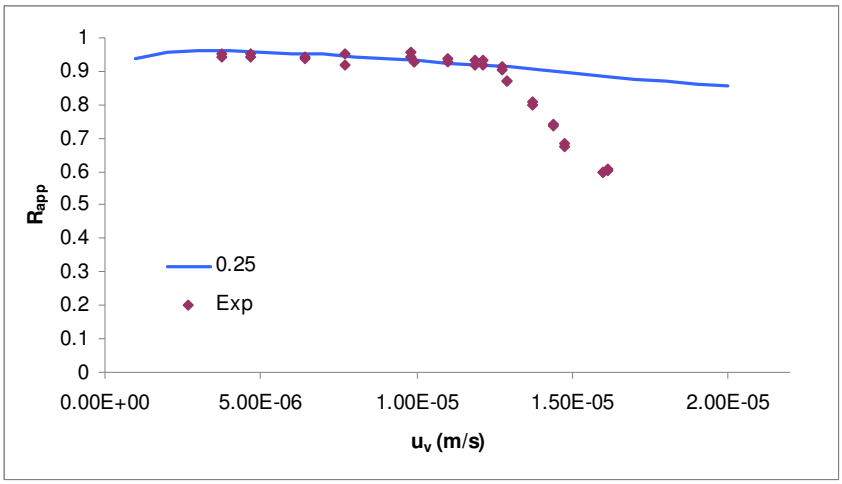

Figure 3. Apparent solute rejection profiles: u_t = 1.57 m/s, K_{eq} = 0.25.

The problem stated above becomes more notorious for results concerning u_t=0.76 m/s. In this case the decrease in rejection occurs earlier and in much stronger manner (vd. Figure 4). Again, the model can successfully replicate experimental results in the high plateau region with the same K_{eq} value, but fails to fit the sudden decrease.

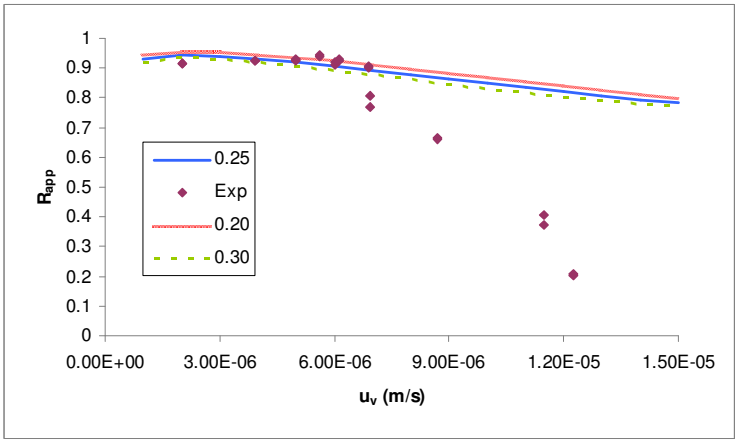

Figure 4. Apparent solute rejection profiles: u_t = 0.76 m/s, for various K_{eq}.

These discrepancies may be due to two major reasons: phenomenon driven, main phenomena enter a different regime in which the model considerations become no longer valid; or parameter driven, the assumptions concerning parameter non-variance in the problem conditions are invalidated. Considering the later case, two important parameters able to affect considerably the results are: membrane resistance, R_m and equilibrium constant, K_{eq}. R_m is estimated using Pure Water Filtration (PWF) experiments in the same conditions (vd. Figure 5; in this case, $R_m = 5.1394 \times 10^{12}$ m^{-1}), a questionable procedure since it is noticeable a typical lack of reproducibility of this kind of PWF data (Blox, 2003). For PEG-3400 filtration experiments this procedure seems to be acceptable, because the experimental pressure drop profiles are very similar to the PWF profiles (Brito et al, 2004). However this is clearly not the case in Dextran experiments. On the other hand, K_{eq} is assumed constant and it is the sole parameter tuned to fit the experimental data available, as stated above. Therefore, it is chosen to test the sensitivity of the model toward these two parameters in order to explain the sudden rejection drop.

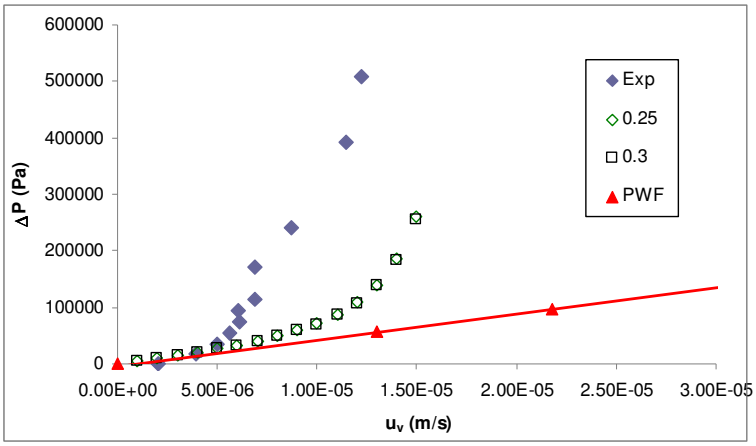

Figure 5. Total pressure drop profiles: u_t = 0.76 m/s, K_{eq} = 0.25; 0.30. (PWF- Pure Water Filtration)

It could be argued that this dramatic rejection drop would be due to sudden changes in the membrane geometry or structure. However, this behavior suggests an important drop in membrane resistance R_m, which is inconsistent with the also dramatic increase in the pressure drop that occurs simultaneously with the rejection fall (vd. Figure 5). In general, this pressure drop rising should be connected with a resistance increase. The same conclusions could be driven by the analysis of the model behavior to changes in K_{eq}. Changing these parameters values in the right direction to account the rejection evolution, will decrease its fitness of pressure data. Alternatively, the pressure drop rising conjugated with rejection drop could be explained with massive solute build-up at the membrane interface leading to extremely high solute concentration values (much higher than the computed by the model in these conditions – up to 25 times the bulk concentration). So, the pressure drop dramatic increase would be due essentially to the osmotic contribution. The model provides a rise in pressure drop and the osmotic pressure drop contribution increases significantly for higher fluxes but overall this rise is insufficient to follow the experimental data. Similar conclusions could be drawn by the analysis of the u_t =1.57 m/s experimental data, which are not presented here. Therefore, it is concluded that the behavior observed is explained by phenomenogical features that are not successfully represented by the model used in the rejection drop zone, and that are particularly visible for lower values of u_t.

5 Conclusions

It is concluded that the model successfully simulates experimental data in the high rejection/low flux region, but it is unable to replicate the observed rejection drop/pressure build-up which occurs for increased fluxes, which may be due to phenomenogical reasons or limitations of the model itself.

References

Blox, M. (2003). Ultrafiltration of multicomponent systems, *Interim Report*, Separation Processes and Transport Phenomena Group, Eindhoven University of Technology.

Brito, P.M.P., Portugal, A.A.T.G. (1998). Application of adaptive methods based on finite difference discretizations in the simulation of a tubular reactor system. *Proceedings of ACOMEN'98 – Advanced Computational Methods in Engineering,* Ghent, Belgium, 697-704.

Brito, P., Ferreira, L.M., Portugal, A., Blox, M., Kerkhof, P. (2004). Modelização de separações por membrana através de métodos de refinamento de malha. *Proceedings of Congresso de Métodos Computacionais em Engenharia*, Lisboa, Portugal, 473 & CD-ROM

Ferreira, L.M., Brito, P., Portugal, A., Blox, M., Kerkhof, P. (2003). A simulation study on the transport phenomena in ultrafiltration. *Workshop on Modelling and Simulation in Chemical Engineering*, Coimbra, Portugal, 8 p.

Kerkhof, P.J.A.M. (1996). A modified Maxwell-Stefan model for transport through inert membranes: the binary friction model. *Chemical Engineering Journal*, 64, 319-343.